Proceedings of Ninth World Conference on Earthquake Engineering
August 2-9, 1988, Tokyo-Kyoto, JAPAN (Vol.III)

4-3-20

SHAKING TABLE TEST AND NUMERICAL SIMULATION ON NONLINEAR RESPONSE OF SATURATED DENSE SAND

Junichi TOHMA[1] , Keizo OHTOMO[1] ,
Mamoru KANATANI[1] and Nobuyasu KAWAI[2]

[1] Abiko Research Laboratory, Central Research Institute of Electric Power Industry, Abiko-shi, Chiba, Japan
[2] Okumura Corporation, Minato-ku, Tokyo, Japan

SUMMARY

The behavior of saturated dense sand subject to earthquake excitation is examined through large shaking table tests and triaxial compression tests. Evidence for cyclic mobility in the model ground is confirmed by the triaxial tests using undisturbed samples from the ground. An efficient and practical effective stress analysis method is demonstrated by comparing simulated results with those of the triaxial test and the shaking table test.

INTRODUCTION

This paper presents study for evaluating stability of saturated dense sand subject to strong earthquake excitation. Generally , dense sand layer is not considered to be liquefied. It becomes, however, necessary to evaluate generation and dissipation of excess pore water pressure in the ground when extremely strong motion is taken as the design earthquakes for the vital structures such as nuclear power plant buildings. This paper discusses a large shaking table test, triaxial test of its samples, and numerical simulations by effective stress method taking cyclic mobility of the dense sand into consideration.

SHAKING TABLE TEST

<u>Soil container</u> A cylindrical soil container was developed for the shaking test of model ground. The height of the container is equal to 3.0m and is the same as its diameter. The wall of the container is made of 20mm thick rubber so that it may deform along with the deformation of the internal model ground. The cylindrical wall of rubber is stiffened by aluminum rings which resist against soil pressure of internal model ground. The weight of the container structure is about 3000 kg , which is several percent of internal ground. Therefore, the influence of inertia force of the container may be negligible to the model ground motion.

Model ground TONEGAWA SAND is used for the model ground. Mean grain size is 0.34mm, and uniformity coefficient is 1.95. At first the container is filled with water ,then the sand was dropped into the water. In order to make dense sand layer, the model ground was shaken at every 50cm height by the shaking table until the 3m -high saturated ground was completed.

Accelerometers, pore water pressure gages, and shear strain gages are installed along with the center line of the ground as shown in Fig. 1. The relative density ,Dr, of the ground is 70-80%.

Test results The model ground was shaken under various kinds of input motions such as frequency sweep excitation with small amplitude, large sine wave excitation with constant frequency, and synthetic earthquake time histories.

Fig. 2 represents the typical results under continuous sine wave excitation. The frequency and the amplitude of the excitation are 2Hz and 0.4G, respectively, and the duration is 12.5sec ,which corresponds to 25 cycles.

It is seen that the acceleration amplitude gradually increase. The shape of the acceleration record is somewhat different from the original sine wave pattern. It should be noted that the peak value of the time history is very sharp. The excess pore water pressure record just below the accelerometer shows higher frequency than that of the acceleration. The large amplitude toward the negative is characteristic. It can be seen that two cycles of water pressure correspond to one cycle of the acceleration. The positive envelope of the water pressure time history gradually increases. This corresponds to the decrease of the effective stresses in the model ground. It is seen that the envelope finally reaches the initial vertical effective stress. If the relative density of the ground is low ,this condition may be recognized as the liquefaction. But it is not the case in the dense sand. Shear strain time history is also recorded. The amplitude of the strain gradually increases. However, it should be noted that the strain never flow during the excitation. The amplitude of the strain is limited. This fact indicates that liquefaction did not occur in the model ground.

Based on the time histories obtained in the model ground, the effective stress path and stress-strain hysteresis are drawn as Fig. 3 and Fig. 4, respectively. The shear stress in both figures are approximately derived from the acceleration record multiplied by the overburden soil mass. Effective stress is defined as the difference between the excess pore water pressure and the initial vertical effective stress. It is seen that the effective stress path moves cyclically along with the inclined lines which may be considered as failure lines. The failure angle can be determined to be 25 ° as indicated in Fig. 3. As can be seen, the effective stress increase along with this line as long as the shear stress is being applied. The hysteresis shows a hard-spring type loop. In other expression, the increase of the strain may be limited in a high shear stress regime. It is seen that the double amplitude of the strain is less than 2%. This may be almost the ultimate strain in this model ground.

TRIAXIAL COMPRESSION TEST

Method Triaxial compression tests were performed for the saturated dense sand. Undisturbed block samples for the tests were taken from the model ground with special care. The samples were taken at three different depths; GL-25cm, -125cm, and -225cm. A total of 13 cylindrical specimen was taken from the block samples by use of a trimmer in a frozen state. The diameter of the specimen is 9.6cm, and the height is 20cm.

It should be emphasized that the triaxial tests were performed under very low confining pressure which corresponds to the model ground. For example, the confining pressure is 0.124 kgf/cm^2 (12.4 KN/m^2) for the sample from GL-125cm depth. Thus, the confining pressure dependent soil properties are directly obtained for the model ground.

Effective stress path Effective stress path are drawn based on the time history record of both excess pore water pressure and applied shear stress to the specimen. A representative path is shown in Fig. 5, where failure lines are obviously appeared. It is seen that the path is increasing and decreasing cyclically along with the failure line. The angle of the failure line is determined as 35°. Conversion of the failure angle determined from the triaxial test to actual ground may be written as:

$$\tan\phi' = \frac{1 + 2K_0}{3} \tan\phi \qquad (1)$$

where, ϕ' : The failure angle for shaking table test(=25°)
ϕ : The failure angle for triaxial test(=35°)
K_0 : Coefficient of earth pressure at rest

Assuming the value of K_0 to be 0.5, it can be seen that the failure angle is converted by eq.(1).

In dense sand, evaluation of failure angle is important because excess pore water pressure build up is controlled by the failure lines as shown in Fig. 3 and Fig. 5.

NUMERICAL SIMULATION

Pore water pressure evaluation The empirical formula by Seed;

$$r_N = \left(\frac{1 - \cos \pi r_u}{2}\right)^{\alpha} \qquad (2)$$

is implemented to evaluate step by step increase of pore water pressure. Where, $r_N = N/N_l$, $r_u = u/\sigma_{mi}'$.
The relationship of number of loading, N, and applied stress ratio, R_l, can be expressed as;

$$\frac{N_l}{20} = \left(\frac{R_l}{R_{l\,20}}\right)^{\beta} \qquad (3)$$

Using eq. (2) and (3), Kokusho established an algorithm for pore water pressure build up calculation taking cyclic mobility into account(Ref. 1). Annaki's concept of cumulative damage is utilized to account for the irregurality of the applied stress history(Ref. 2).

Cyclic mobility effect is to be controlled on a shear stress-effective stress plane , i.e., effective stress path as illustrated in Fig. 6. The effective stress dose not cross the given failure lines. Once the path reaches the failure line, the effective stress is controlled to be increased along with the line as long as the shear stress is being applied. Thus, cyclic change in sign of pore water pressure history can be simulated.

Simulation of triaxial test In order to confirm the algorithm for the dense sand used in the shaking table test, the triaxial tests were simulated numerically as follows.

Assuming $\alpha=2$, $\beta=-5$, $\phi=35°$ and $R_{l\,20}=0.8$, the pore water pressure time history was obtained under sine wave stress as shown in Fig. 7. The simulated effective stress path is also shown in Fig. 8 . It can be seen that the stress path approximately consistent with the triaxial one(Fig. 5)

Simulation of shaking table test A stick model is constructed to simulate the model ground as shown in Fig. 9. Each element has Hardin-Drnevich type skeleton curve for stress-strain relationship. Masing rule is applied for hysteretic behaviors. A direct integration analysis is carried out by Newmark's β method. It is noted that stress and strain are normarized by effective mean stress at each time step. The effective mean stress is calculated from pore pressure which is generated at each time step. Thus, effective stress analysis can be performed. The simulated maximum pore water pressure build up is compared with experimental results under EL CENTRO excitation(time scale factor 1/5, maximum acceleration 0.3G). The comparison is shown in Fig. 10 . Simulated values agree well with the experimental results. Note that the pore water pressure build up is moderate reflecting high strength to liquefaction.

CONCLUSION

Large shaking table test and triaxial compression test were performed to evaluate cyclic mobility of the dense sand. Both results are consistent. A practical effective stress method simulates numerically the pore pressure build up in the dense sand taking the cyclic mobility into consideration.

REFERENCES

1. Kokusho, T., Liquefaction Analysis Compared With Shake Table Test, 8th WCEE, Vol. Ⅲ, pp. 135-142, (1984).
2. Annaki, M. and Lee, K. L., Equivalent Uniform Cycle Concept for Soil Dynamics, Proc. ASCE, Vol. 103, GT6, (1977).

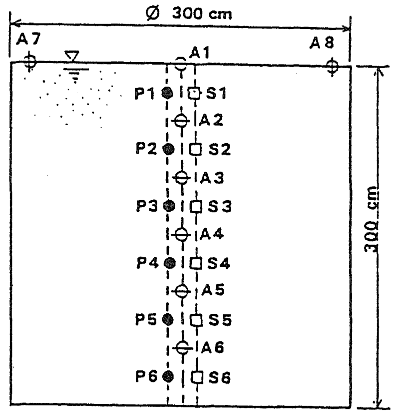

ACCELEROMETER
PORE WATER PRESSURE GAGE
SHEAR STRAIN GAGE

Fig. 1 THE MODEL GROUND

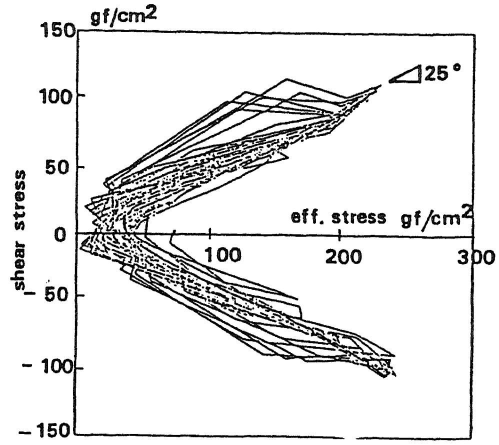

Fig. 3 EFFECTIVE STRESS PATH FROM THE SHAKING TABLE TEST

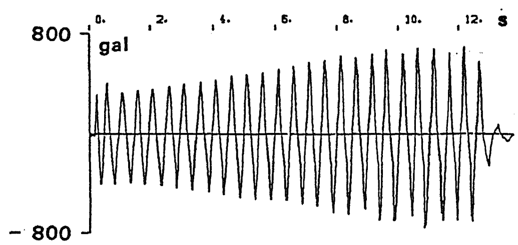

(a) ACCELERATION RECORD OF [A2]

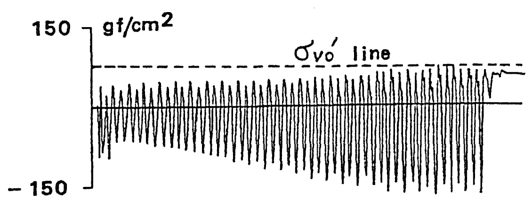

(b) WATER PRESSURE RECORD OF [P2]

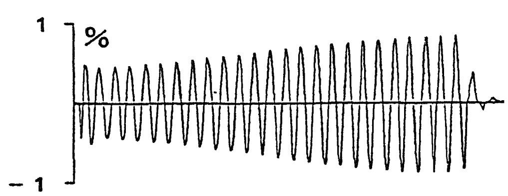

(c) SHEAR STRAIN RECORD OF [S2]

Fig. 2 RESULTS OF THE SHAKING TABLE TEST

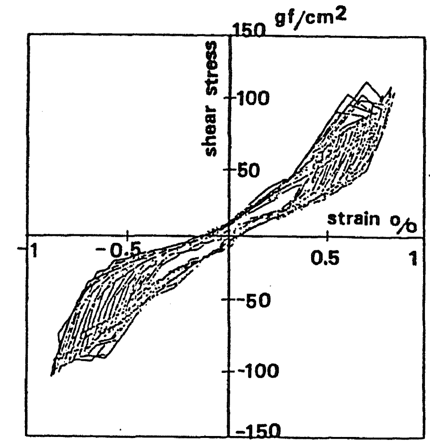

Fig. 4 STRESS-STRAIN HYSTERESIS FROM THE SHAKING TABLE TEST

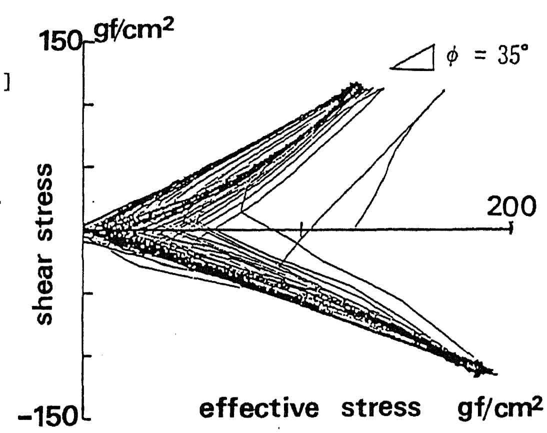

Fig. 5 EFFECTIVE STRESS PATH FROM THE TRIAXIAL TEST

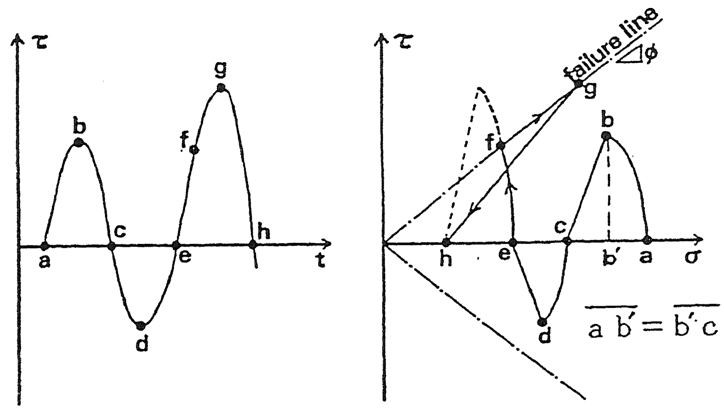

(a) APPLIED STRESS HISTORY (b) EFFECTIVE STRESS PATH

Fig. 6 EFFECTIVE STRESS MODEL

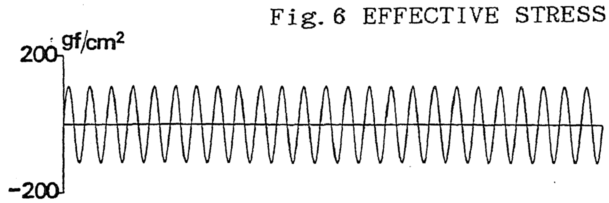

(a) APPLIED STRESS HISTORY

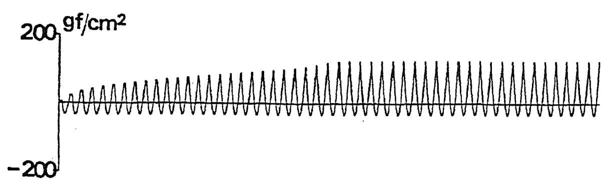

(b) CALCULATED PORE WATER PRESSURE HISTORY

Fig. 7 SIMULATED TRIAXIAL TEST
BY THE NUMERICAL MODEL

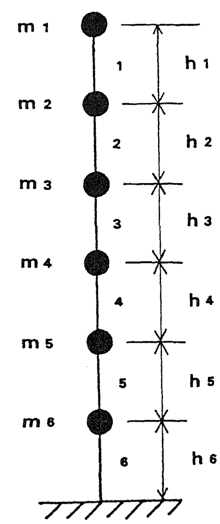

Fig. 9 A STICK MODEL FOR
THE MODEL GROUND

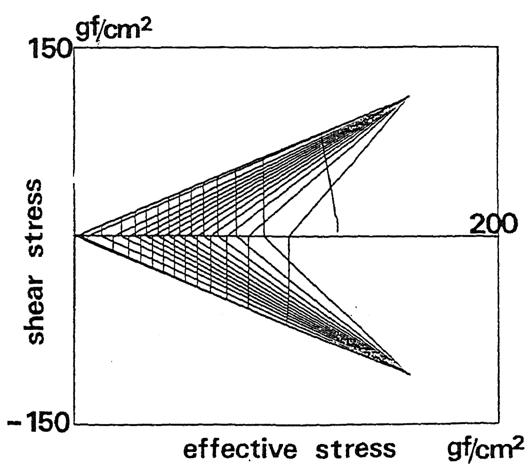

Fig. 8 SIMULATED EFFECTIVE STRESS PATH
BY THE NUMERICAL MODEL

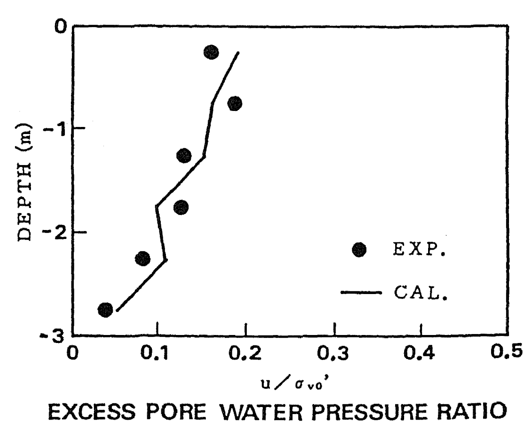

Fig. 10 COMPARISON OF PORE WATER
PRESSURE BY EXP. AND CAL.